HEAT RADIATION OF BURNING HYDROGEN/AIR MIXTURES IMPURIFIED BY ORGANIC VAPOUR AND PARTICLES

Weiser, V., Roth, E., Eckl, W., Kessler, A., Langer. G
Energetic Systems, Fraunhofer Institut für Chemische Technologie (ICT), Joseph-von-Fraunhofer-Str. 7, 76327 Pfinztal, Germany, volker.weiser@ict.fraunhofer.de

ABSTRACT

Experiments were performed to investigate the radiative heat emission of small scale hydrogen/air explosions also impurified by minor amounts of inert particles and organic fuels. A volume of 1.5 dm^3 hydrogen was injected into ambient air as free-jet and ignited. In further experiments simultaneously inert Aerosil and combustible fuels were injected into the blasting hydrogen/air gas cloud. Fuels were a spray of a solvent (Dipropyleneglycol-methylether) and dispersed particles (milk powder). The combustion was observed with a DV camcorder, an IR camera and two different fast scanning spectrometers in NIR and IR range using a sampling rate of 100 spectra/s. The intensity calibrated spectra were analyzed using ICT-BaM code to evaluate emission temperature and intensity of H_2O, CO_2, CO, NO and soot emission. Using the same code combined with the experimental results total heat emission of such explosions was estimated.

INTRODUCTION

Hydrogen burning in air emits heat radiation effected by broad water bands in NIR and IR spectral range. Especially, in the case of large cloud explosion, the risk of heat radiation is commonly underestimated due to the non-visible flame of hydrogen-air combustion [1]. In realistic industrial cases explosion accidents will occur accompanied by the co-combustion of minor amounts of organic substances. So additional soot and carbon oxide will be produced that increase total heat radiation substantially. In the recent safety discussion of hydrogen the question was asked on similar risk of smaller gas clouds that may be evolved e.g. from leakages of fueling systems.

The purpose of this study was to estimate the heat radiation emitted from small scale hydrogen-air explosions also impurified by minor amounts of inert particles and organic fuels in liquids and solid state. To achieve this aim more than 50 gas explosions of 1.5 dm^3 hydrogen were performed under different conditions regarding time and position of ignition and co-combustion of dispersed fuels. The experiments were investigated using an IR-camera and two fast scanning spectrometer. The emitted heat radiation was interpreted also using modeling data of spectral radiation.

EXPERIMENTALS

Set-up

During 300 ms a hydrogen volume of 1.5 dm^3 (273 K, 0.1013 MPa) was released out of a container (volume 3.9 dm^3 and initial pressure 0.25 MPa) into free air. Ignition was achieved using periodic initiated electric sparks in various horizontal and vertical distances from the nozzle. The set-up was part of investigations described in ref. [2] performed to investigate ignition phenomena. In a second series of experiments a defined amount of particles and liquid droplets were injected simultaneously into the hydrogen/air free jet in cross-flow using various amounts and injection pressures.

Particles injected into the hydrogen/air mixture consist in three types of species:

1) Aerosil 200 (DEGUSSA). Example of fine inert particles. Highly agglomerated nano-particles of a silicic acid (SiO_2 n H_2O). In thermo analytical experiments it was validated that Aerosil do not to react with air. So it was assumed to be inert during the explosion. 0.5 and 1.5 g were injected into the hydrogen/air cloud.

2) Dowanol DPM (Dipropyleneglycol-methylether). Example of organic fuel. A chemical solvent ($CH_3O[CH_2\text{-}CH(CH_3)O]_2H$) manufactured by DOW Chemicals that is completely mixable with water; boiling point 463 K; flash point 348 K; heat of combustion 27.2 kJ/kg. In all cases 4 ml DPM were injected as spray.

3) Milk powder. Example of organic particles. Produced by Schwarzwaldmilch with 26% fat and 3.55% water. For combustion calculations a sum formula of $C_1H_{1.86}N_{0.08}O_{0.53}$ can be assumed. Additional elements are K, Ca, Cl and Na (total about 0.1 ma%) and additional trace elements (<<0.1 ma%). This milk powder decomposes endotherm in two main steps at 190°C and 320°C forming coke particles of about 50 µm. In air combustion starts at 450°C. Decomposition and combustion of milk powder clouds is investigated in more detail in [8], [9]. Amounts of 5 and 10 g were injected into the cloud.

In this reported study the parameter variation aimed for the determination of worst-case amounts of heat emission from the exploding gas clouds and is not purpose of a detailed discussion.

Measurement techniques

DV-camera

The visual flame shape was observed with a digital video camcorder (Panasonic NV-DX110). By separation of the even and odd interlaced frames a time resolution of 50 frames/s with an optical resolution of 720 × 288 pixels was achieved.

IR-camera

An IR-camera of FLIR SC500 recorded images of the radiation in the MIR-spectral range of 7.5 to 13 µm. The pixel resolution of 320 × 340 and the frame rate of 50 s^{-1} were just sufficient to observe the geometric scale of flame zone.

NIR-spectrometer

A fast scanning hot gas sensor (HGS) based on a Zeiss MCS 511 NIR spectrometer was used [3]. It is a grating spectrometer with an InGaAs diode array as detector (spectral range 0.9 to 1.7 µm). The spectral resolution is about 15 nm at a scan rate of 300 spectra per second. A 600 µm glass fibre is used as optical entrance. With a pin hole in front of the fibre the field of view was reduced to an angle of 7°. The fibre was placed close to the ejecting nozzle and was adjusted about 0.1 m above the ignition point where maximum flame reaction was assumed.

IR-spectrometer

A filter wheel spectrometer consists of a fast rotating wheel with three interference filter segments. They continuously vary the transparency in the wavelength regions 2450 to 14000 nm (InSb/HgCdTe-sandwich-detector) [4]. The system allows up to 130 turns per second. On each turn one complete spectrum is achieved. On the recent study 100 turns per second were used. The optic structure consists in an “infinity to 1” projection realized by ZnSe-lenses. The spectrometer was adjusted to the position of ignition.

For intensity calibration of all spectrometer systems a technical black body radiator was used. But it is to consider that this calibration only results in a value of intensity per wavelength. Therefore the

applied optics did not result in a defined field of view no calibration concerning to emitting area and steradian was possible, so the absolute intensity can not be compared.

BaM-Code Evaluation

For spectral radiation modeling ICT-BaM Code was used [5]. It was also used to determine physical properties like temperature or optical depth from emitting and absorbing chemical species from recorded spectroscopic data. For both the wavelength resolved intensity distribution has to be modeled and compared to experimental spectra. The calculation of molecular emission and transmission spectra needs the knowledge of the temperature and wavelength resolved absorption coefficient. Non-linear polyatomic molecules like water have lots of spectral lines in the infrared which cannot be calculated applying a simple analytical model [6]. Therefore, a band model, based on tabulated data must be used considering profile, half width and distribution of spectral lines. At high temperatures, the ‚Random Band Model‘ with a combined Doppler and Lorentz profile is approved. Additionally, each molecule is compressed in a line group (Single-Line-Group-Model). The Curtis-Godson-Approximation is used to get the ‚Curve of Growth‘.

The here applied modeling code ICT-BaM of the near infrared water band spectra is based on the data published in the ‘Handbook of Infrared Radiation from Combustion Gases’ [7]. It allows the calculation of the emission and transmission spectra of H_2O, CO_2, CO, NO and HCl in a temperature range from 600 to 3500 K taking into account self absorption, pressure broadening and soot. Also grey body radiation with a constant emissivity can be introduced. The calculated intensity distributions are compared to experimental spectra by a least-squares fit routine with the parameters temperature and concentration × path length. An example for the data analysis is shown in Figure 5 and Figure 9. A more detailed description of the band modeling theory is given in [5].

RESULTS

Visual picture

As assumed no visible emission can be observed from pure hydrogen/air explosion (Figure 1a). Only when watching the movies ascending schlieren can be noted ascending upward in front of the back ground structure like used in [10] to investigate the ignition and the combustion front of the gas explosion. If inert Aerosil is inserted into the blasting gas zone only a dark red emission can be noted during the explosion (Figure 1b). The injection of the liquid DPM fuel spray results in a weak yellow flame appearing during the blast (Figure 1c). If the H_2/air explosion is mixed with an injected fuel dust (milk powder) an intensive co-combustion with a bright yellow flame can be detected (Figure 1d). It is larger than the reaction zone of the pure hydrogen/air mixture. That shows a comparison with simultaneously received thermographs (e.g. Figure 3). Each presented pictures represent the most intensive and largest flame of all measurements.

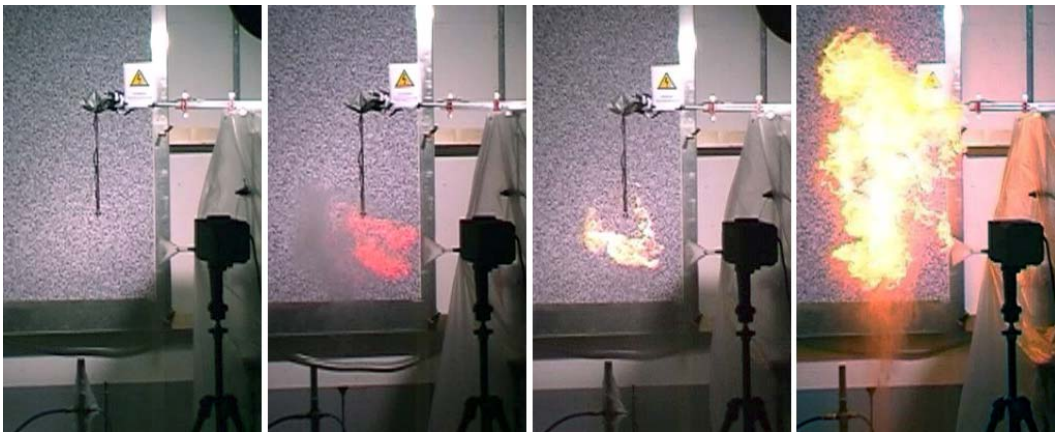

Figure 1 DV camera prints of hydrogen/air explosions a) pure, b) plus Aerosil, c) plus DPM, d) plus milk powder (pictures with maximum emission)

Thermographs

Thermographs were used to estimate the position and volume of the emitting combustion zone. The detector sensitivity from 7.5 to 13 µm covers some optical thick water bands between 6 and 10 µm and continuous emission from particles e.g. soot (compare Figure 9). So it is applicable to visualize a non-luminous flame of hydrogen or hydrocarbons. But one has to take into account that no carbon oxide emission is covered (CO_2 at 2.7 and 4.3 µm, CO at 4.2 to 5.4 µm).

The IR-movies show that the part of reaction including the most intensive heat emission takes place close to the point of ignition. Afterwards the flame zone quickly ascent upward but simultaneously decreases in temperature and intensity (compare Figure 2). So it can be assumed that the field of view of the spectrographs covers the position of highest heat emission. Only in the case when ignition was performed at the border of the gas cloud in an area with lean stoichiometry the highest emission was elsewhere. But the thermographs approve that in this cases the total reaction was weak and the flame size and emission intensity were very low compared to the other cases.

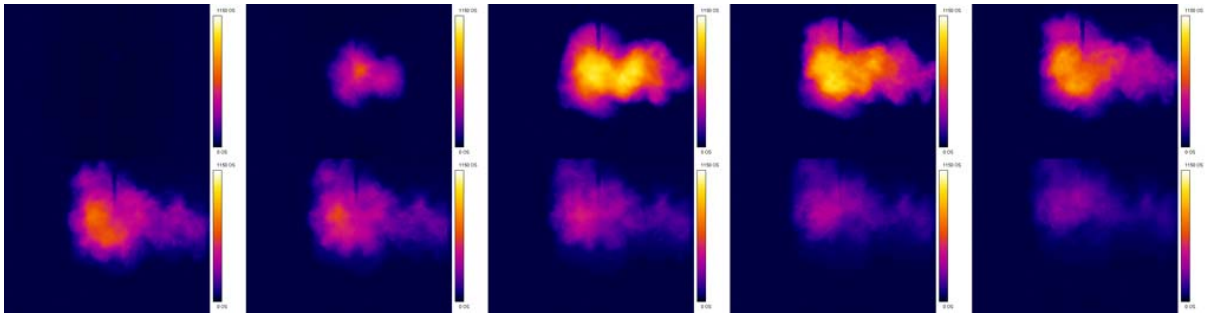

Figure 2 Sequence of thermographs resulting from a pure hydrogen/air explosion

According to Figure 1 the exposures of the most intensive and largest reaction zones of all measurements are arranged in Figure 3 using the same scale and colour code to present the intensity of radiation for all exposures. It is obvious that the size of flame differ not very much in all cases. Taking into account the thermographs of all IR-camera movies it is validated that the main part of the heat radiation was emitted from approximately a ball of about 400 mm diameter. Only the explosion with 10 g milk powder (Figure 3d) was significant larger and may be described with a ball of 500 mm. When the cloud was charged with droplets or particles the maximum intensity of emission (white spots in Figure 3b to d) is higher than that from the pure hydrogen/air explosion. The calibration of the IR-detector conducted from the manufacturer did not allow to estimate the absolute ratio.

NIR-spectra and temperature

In the investigated NIR-range only water bands and particle radiation could be detected. Figure 4 shows spectra sequences taken from a pure hydrogen/air explosion (a) and the most intensive explosion including 10 g milk powder (b). The pure hydrogen/air explosion emits only water with bands at 0.95, 1.15 and 1.4 µm. The co-combustion of milk-powder also generates an intensive soot continuum. Lines at 1.18 and 1.25 µm indicate 2nd order diffraction from potassium and calcium. The sequence of Figure 4b demonstrate that first hydrogen is ignited and then during the heat release milk powder starts to pyrolyse and forming soot particles (compare also Figure 6). This soot emission has a distinct contribution to the total emission.

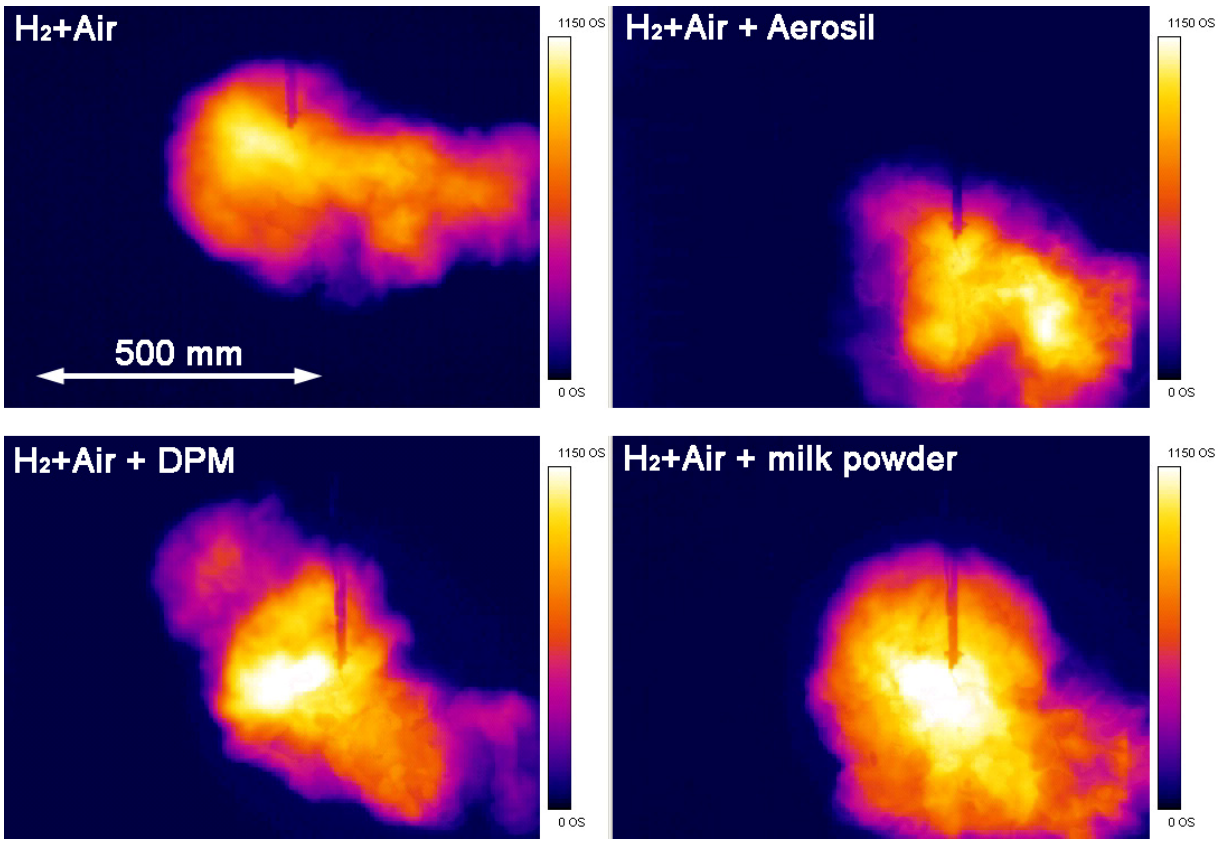

Figure 3 Screenshots from IR-camera of hydrogen/air explosions a) pure, b) plus Aerosil, c) plus DPM, d) plus milk powder (pictures with maximum emission)

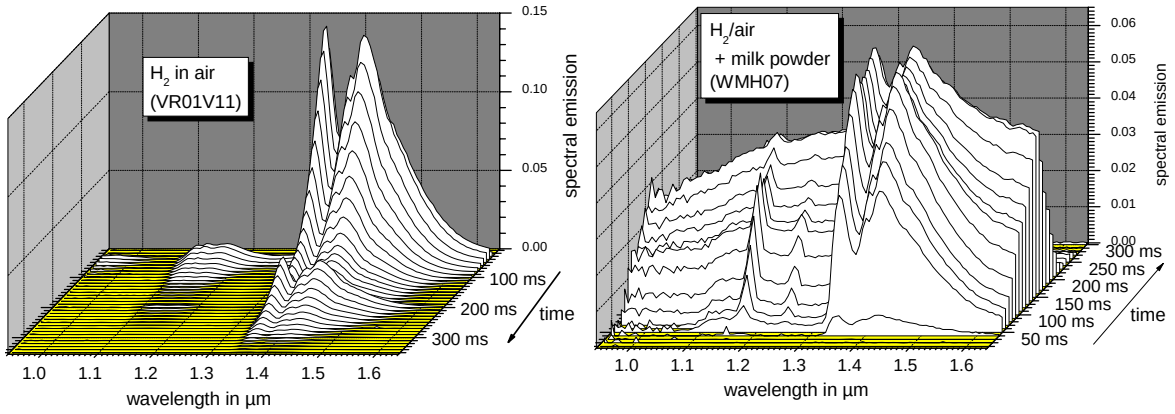

Figure 4 Spectra sequence of a) pure hydrogen/air explosion, b) hydrogen/air impurified with milk powder

The quality of the spectra was good enough for analysing with ICT-BaM-Code. Figure 5 shows an HGS-spectra of each sample type compared with the best ICT-BaM-fit and the received temperature. It was found that the fit is excellent and the resulting temperatures are authentic.

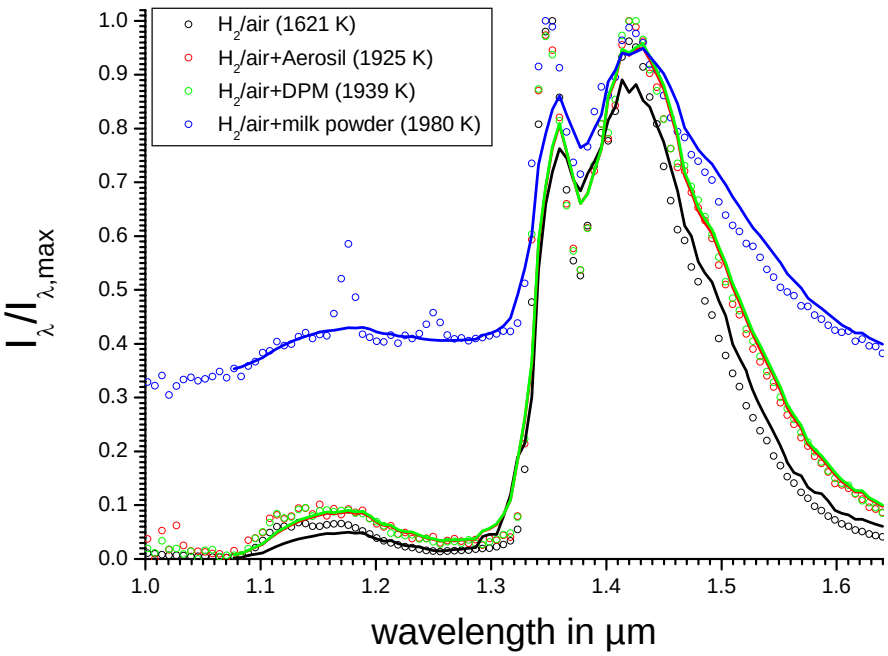

Figure 5 Exemplary NIR-spectra compared with best ICT-BaM-fit for temperature determination (in brackets); spectra normalized with maximum intensity

Analysing all spectra per sequence lead to time histories like presented in Figure 6. The ICT-BaM-analyses results in integrated intensity of each spectrum from 0.95 to 1.65 µm, its temperature and a signal of water bands and soot. The last two signals are “concentration × pathlength” and have the character of a concentration assuming that all emitting species are homogeneously distributed inside the flame. Therefore intensity calibration is not quantitative regarding to emitting area and steradian and the optical pathlength is not known this concentrations can only interpreted over the same spectrum but they give adequate information on the contributions of the species to the total emission.

In most profiles maximum temperature is reached shortly after ignition of hydrogen and degrease afterwards continuously with about 1000 K/s. In all explosions the period of total emission lasted between 200 and 500 ms. In the case of co-combustion of milk powder (Figure 6b) the soot signal indicates clearly when pyrolysis of the particles proceed. In this period the fraction of soot radiation increases strongly. But when observing the intensity signal (green curve) of the same time profile it is obvious that the total emission at least in the investigated spectral range increase only to the same magnitude then the pure hydrogen intensity at the beginning of the reaction.

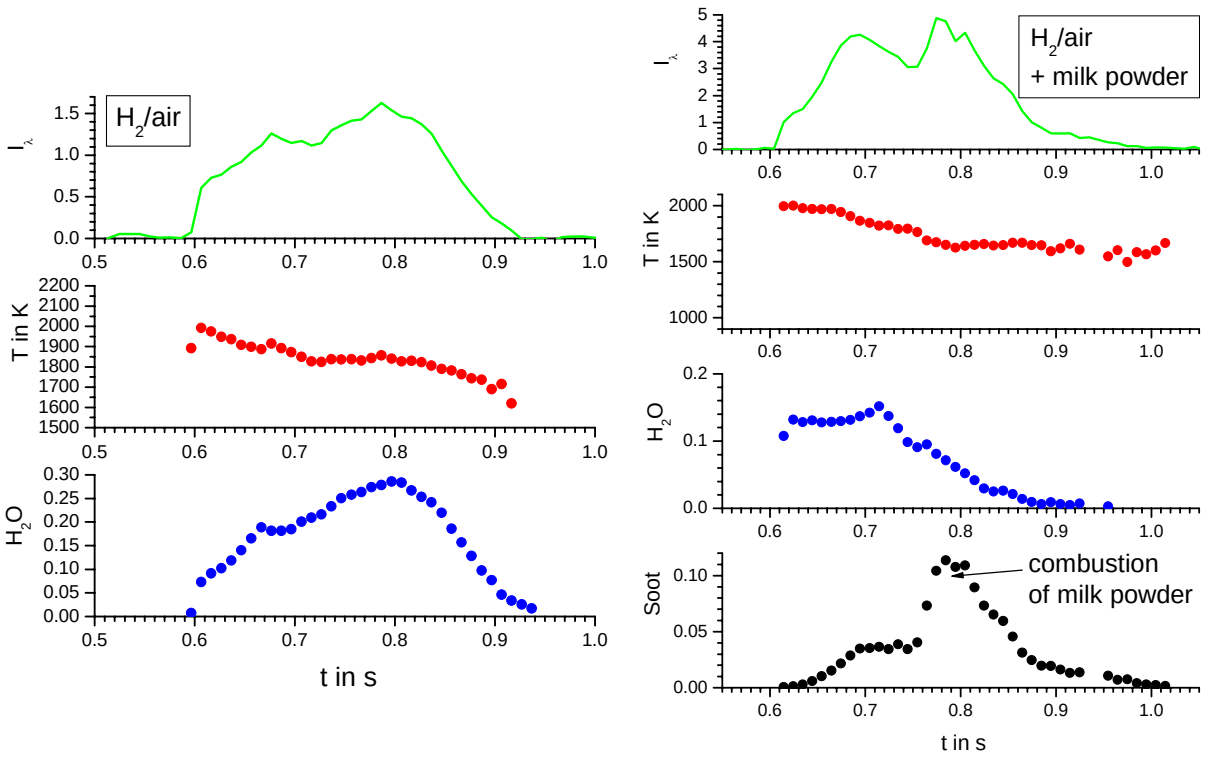

Figure 6 ICT-BaM evaluation of spectra sequences received from the combustion of a) pure hydrogen/air explosion, b) H_2/air plus milk powder

In conclusion to this the most important results of the HGS-signals are the time history of the radiation temperature from the flame ball, which can be accepted without further discussions. In Figure 7 these temperatures are evaluated statistically. Figure 7a show all results averaged over the total reaction time and in Figure 7b the maximum temperatures are compiled. The open dots in both figures indicate values received from experiments when the hydrogen/air mixture did not react completely due to ignition was to late before the gas cloud diluted strongly or ascend driven by buoyancy. The mean temperatures of the pure hydrogen/air explosions are highest. Those of the reaction with inert Aerosil are lowest. This may be explained by the consumption of heat when the inert Aerosil particles were heated and melted. The mean temperatures of combusting fuels DPM and milk powder are in between according to the heat of combustion that is lower than that of hydrogen. Also heat loss by higher radiation may act a part. The maximum temperatures of all samples are in the order of 2000 K reflecting the pure hydrogen combustion (Figure 6).

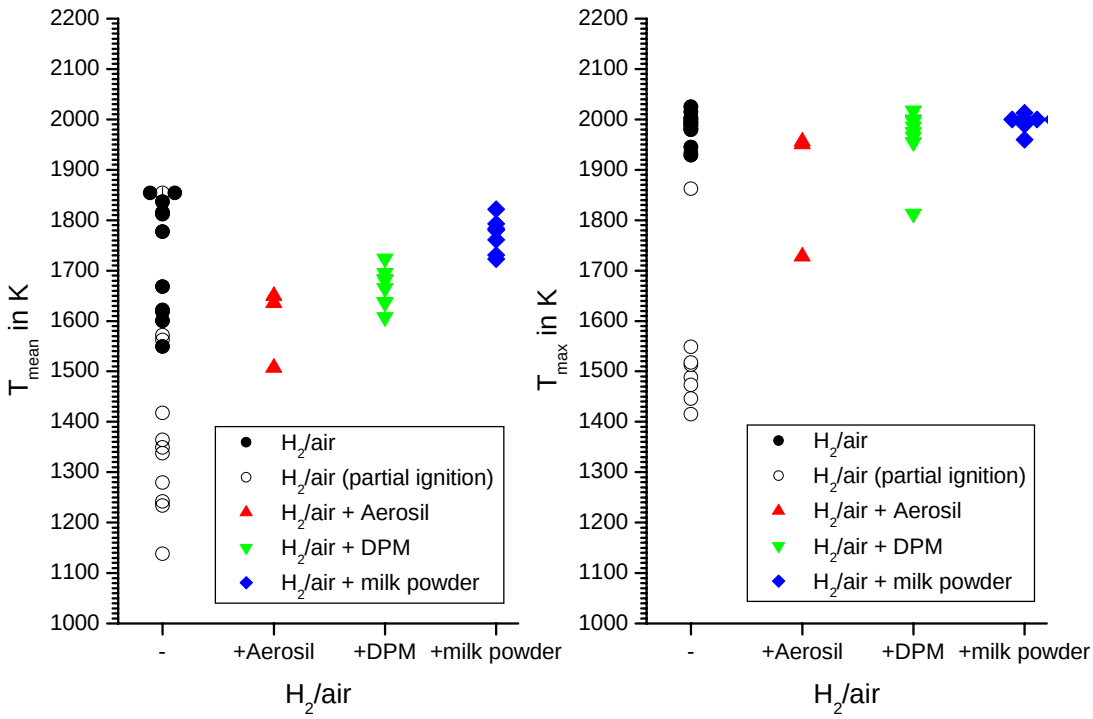

Figure 7 Mean temperatures (left) and maximum temperatures (right) of all experiments

IR-spectra

For more detailed information of emitting species the received filter wheel spectra in medium IR-range were consulted. In Figure 8 two characteristic sequences of spectra are presented. Figure 8a is taken from pure hydrogen/air explosion. Figure 8b results from a H_2/air explosion mixed with 10 g milk powder. This explosion featured the most intensive emission of all experiments also concerning continuum radiation. The time history of intensity shows the same qualitative profile than the NIR-spectra. Main differences consist in additional species only emitting in this spectral range.

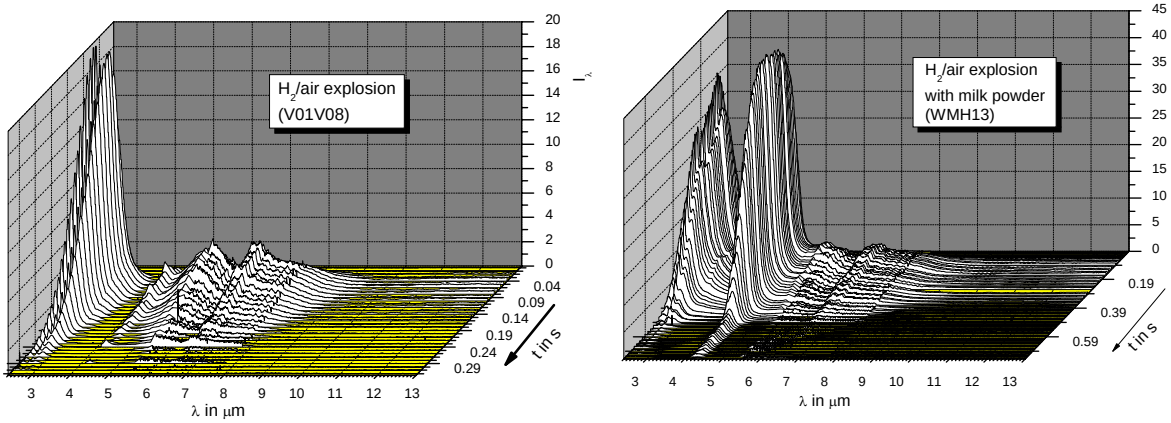

Figure 8 Plot of spectra sequence in IR range of a) pure hydrogen/air explosion, b) hydrogen/air impurified with milk powder

Spectra examples can be regarded in more details in Figure 9. The spectra resulting from an explosion including Aerosil does not differ from a pure hydrogen/air explosion. Mainly water bands are excited. At 4.3 µm a very weak CO_2 emission can be noted. This usually very strong CO_2 band is evoked from

the natural CO_2 concentration in air. The spectra with co-combustion of hydrocarbons show much stronger CO_2 emission with a similar intensity than the water band at 2.9 µm. At the spectrum received from the reaction with milk powder additional CO is present at about 5 µm. Only at these spectra some continuum radiation is enclosed that indicate particle emission from soot. It is obvious that both have only a minor contribution to total emission. In Figure 9 also best least-squares fits resulting from an analysis with ICT-BaM are included. The fits are well and validate the resulting parameters.

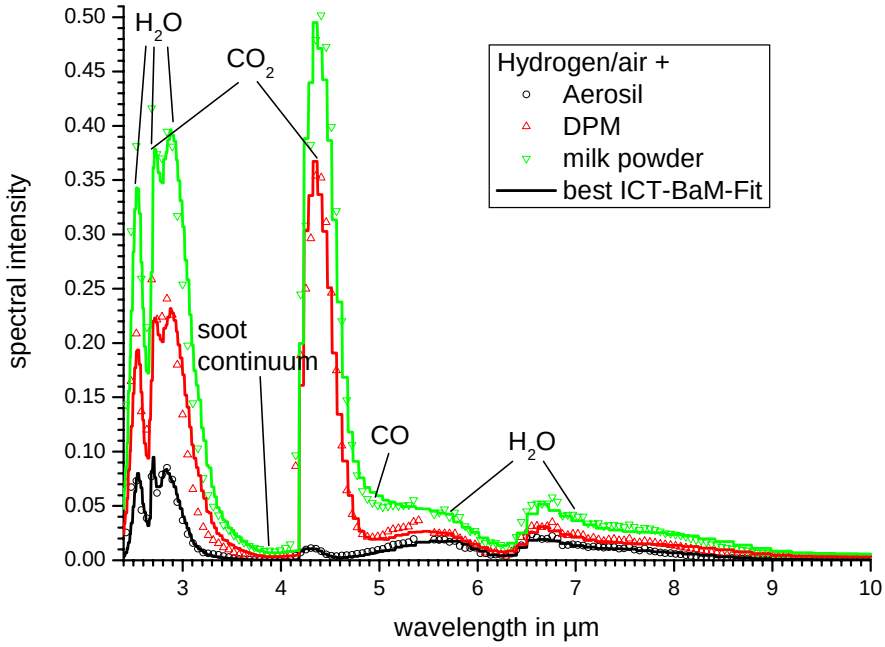

Figure 9 Infra red spectra received from hydrogen/air explosions with additional particles in the combustion zone compared with best least-squares fits resulting from ICT-BaM analysis

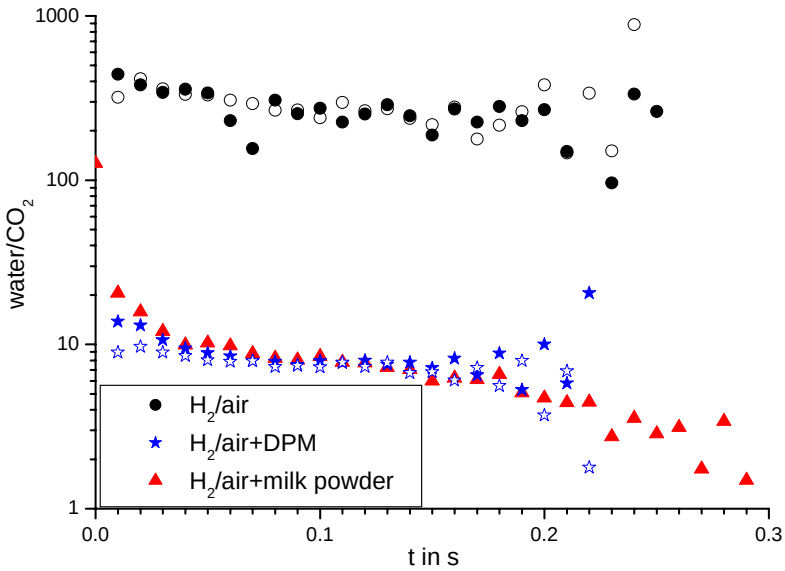

Figure 10 Ratio of concentration length of water to CO_2 resulting from spectra sequences of hydrogen/air explosions partially mixed with DPM and milk powder achieved by ICT-BaM analysis

The resulting temperatures agree well with the HGS analysis. Absolute emissivity is not received by reason that also the IR-spectra are only calibrated in power per wavelength. So the BaM analysis only results in concentrations relative to other emitting species inside the same spectrum like described above. Such results are presented in Figure 10 displaying the development of the molar ratio of water related to CO_2 along the explosion time. It is significant that this ratio do not vary during the reaction. The very high ratio in a magnitude of 500 at pure H_2/air explosions correlates with the statement that here CO_2 is due to the natural concentration in air. In the other cases this ratio is in the dimension of 10 that also will be used for the estimation of total emission intensity.

DISCUSSION

In scope to discuss the radiative heat emission of free hydrogen/air explosions in small scale (1.5 dm^3 H_2) the experimental results can be summarized as follows:

- The reaction of the inhomogeneous mixed hydrogen in air takes place very quickly in a period of about 10 ms forming a hot gas volume that may be described as a sphere of 0.4 to 0.5 m diameter (comp. Figure 2 and Figure 3).
- The gas temperature amounts to 2000 K (Figure 7b).
- In 0.2 to 0.3 s the gas volume cools down to 1500 K without dramatic changes of shape and size (comp. Figure 2).
- Even in the case of co-combustion of organic species the main heat emission is caused by water band systems in spectral range 1 to 9 µm.
- In the case of pure hydrogen/air explosion the contribution of natural CO_2 is negligible. Even in the case of co-combustion of a considerable amount of hydrocarbons the molar fraction of emitting CO_2 does not exceed 10% of water. In the same case the contribution of continuum emission of soot or other particles can be described with a low emissivity of less than 0.02.

To estimate the emitted heat radiation a method know as SEP-model and widely used in fire safety science shall be applied [11]. The flame ball is assumed to be a homogeneous emitting solid sphere with a constant overall emissivity ε defined as:

$$\varepsilon(T) = \frac{\int_{-\infty}^{\infty} \varepsilon(\lambda,T)\, L_S(\lambda,T)\, d\lambda}{\int_{-\infty}^{\infty} L_S(\lambda,T)\, d\lambda} = \frac{\int_{-\infty}^{\infty} \varepsilon(\lambda,T)\, L_S(\lambda,T)\, d\lambda}{\sigma T^4 \Omega_0}$$

L_S is the Planck's function for black body radiation only depending on wavelength λ and absolute temperature T in the units of intensity per (wavelength × emitting area × steradian Ω_0) [12]. ε(λ,T) is the spectral emissivity of the hot gases (e.g. water bands). The total integral of Planck's function is given by the Stefan-Boltzmann T^4-law with $\sigma = 5.67 \times 10^{-8}$ W m^{-2} K^{-4}. ε(λ,T) of the water bands can be calculated e.g. with ICT-BaM code or RADCAL [13].

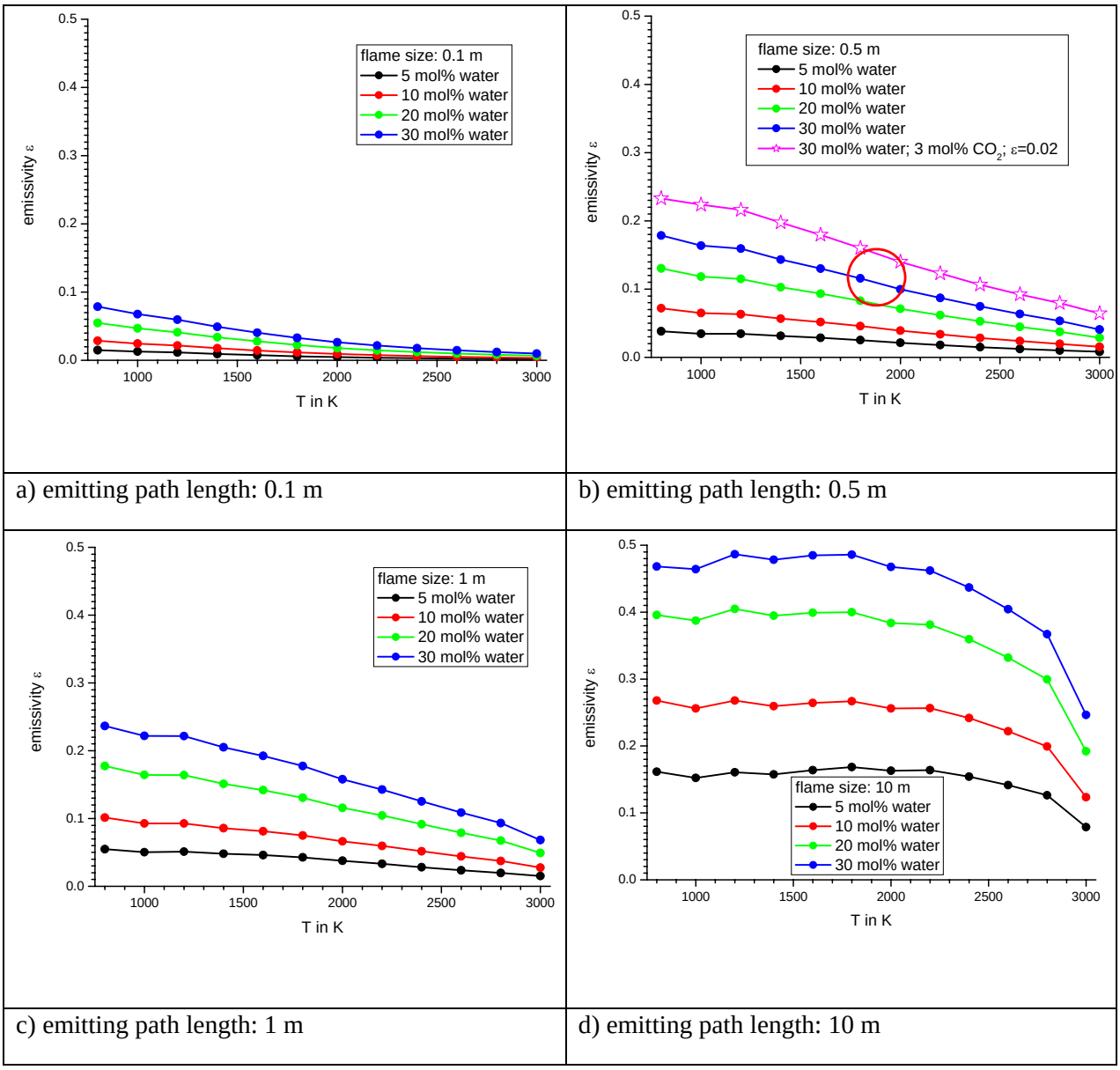

a) emitting path length: 0.1 m

b) emitting path length: 0.5 m

c) emitting path length: 1 m

d) emitting path length: 10 m

Figure 11 Total emissivities of hot water gas calculated with ICT-BaM code as function of temperature, concentration and optic path length. Red circles indicate values fitting to the reported experiments.

Results for ε as function of T are calculated from λ = 1 to 10 µm and are presented in Figure 11 for various path lengths (flame sizes) and water concentrations. Below 3000 K this interval qualifies more than 99.9% of total water emission intensity. Emissivities decrease with temperature and increase with water concentration and path length. Especially at higher concentrations the increases are not linear. At low concentrations and path lengths water acts optical thin but with higher values it becomes more and more optical thick converging black body radiation. A critical value is in the magnitude of 10 m. In Figure 11b with a path length of 0.5 m suitable to our experiments additionally the total emissivity with values for H_2O, CO_2 and soot that were found above is listed. Compared to pure water gas the emissivity is about 50% higher. These values seem small but it should keep in mind that at higher path lengths soot and CO_2 becomes optical thick much faster as water so that in real hazardous explosions very high emissivities will be expected.

Using ideal gas law a sphere of 400 mm at 0.1013 MPa with 2000 K contains about 0.2 mol. Starting from a stoichiometric mixture of hydrogen with air: $H_2 + 0.5\ (O_2 + 79/21\ N_2) \rightarrow H_2O + 79/42\ N_2$ a

stoichiometric mixture of 1.5 dm^3 H_2 with air has a similar mol number of product gases. This corresponds to about 30 mol% water inside the flame ball. So the emissivity of the performed measurements may be assumed with ε=0.15 like indicated in Figure 11c by a red circle. So the heat emission of the flame balls may be estimated of $\varepsilon \sigma T^4$ = 136 kW m^2.

CONCLUSIONS

Small scale explosions of 1.5 dm^3 hydrogen in free air were investigated resulting in flame balls of 0.4 m emitting with 1500 to 2000 K with a total emissivity in the order of magnitude ε=0.15. The injection of co-combusting organic materials increases the emissivity to ε=0.20 with similar temperature. This data do not result in a dangerous heat radiation concerning these small scale explosions. The reported method of investigation is also applicable to study much larger gas explosion which are presumed to emit more dangerous heat radiation.

REFERENCES

[1] V. Weiser; E. Roth; S. Kelzenberg; W. Eckl; N. Eisenreich; G. Langer; Measuring and modelling unsteady radiation of hydrogen combustion; International Conference of Hydrogen Safety (ICHS); Sept. 8-10, 2005; Pisa; Italy; Poster 120047

[2] A. Keßler, V. Weiser, W. Ehrhardt, S. Kelzenberg, G. Langer; Hazards of Accidental H_2-Jet Release Ignition Distances and Impact by Radiation; accepted for this symposium.

[3] Eckl, W.; Weiser, V.; Eisenreich, N.; Spectroscopic Flame Diagnostics by Analyzing NIR Water Bands; 5th International Symposium on Special Topics in Chemical Propulsion: Combustion of Energetic Materials; 19-22 June 2000; Stresa, Italy; paper 5-ISICP-007-9-OP-VW

[4] Blanc, A.; Eisenreich, N.; Kull, H.; Liehmann, W.; "Charakterisierung von Verbrennungsprozessen mittels zeitaufgelöster IR-Spektroskopie im Bereich 1 - 14 µm", 19th Int. Annual Conf. of ICT, Karlsruhe, June 29 – July 1, 1988, pp. 74/1 – 74/15

[5] Weiser, V.; Eisenreich, N.; Fast emission spectroscopy for a better understanding of pyrotechnic combustion behaviour; Propellants, Explosives, Pyrotechnics 30, 67-78, 2005

[6] Herzberg, G.; "Molecular Spectra and Molecular Structure II. Spectra of Polyatomic Molecules", D. van Nostrand Company Inc., Princeton, New Jersey, 1950

[7] Ludwig, C.B.; Malkmus, W.; Reardon, J.E.; Thomson, J.A.L.; Handbook of Infrared Radiation from Combustion Gases, NASA SP-30980 (1973)

[8] V. Weiser, E. Roth, S. Kelzenberg, J. Neutz, N. Eisenreich, U. Hahn; Detektion und Bekämpfung von B- und C-Kampfstoffen (Teil 2), 1. Zwischenbericht zum Forschungsvorhaben E/E210/3D094/Y5166; Pfinztal, August 2004

[9] Weiser, V.; Neutz, J.; Eisenreich, N.; Roth, E.; Schneider, H.; Kelzenberg, S.; Development and characterization of pyrotechnic compositions as counter measures against toxic clouds; 36th International Annual Conference of ICT & 32nd International Pyrotechnics Seminar; June 28 – July 1, 2005; pp. 5-(1-14)

[10] Kessler, A.; Ehrhardt, W.; Langer, G.; Hydrogen Detection: Visualisation of Hydrogen using non Invasive Optical Schlieren Technique BOS. "ICHS 2005" 1st International Conference on Hydrogen Safety, September 9th – 10th 2005, Pisa, Italy

[11] P.J. DiNenno, (ed.); SFPE Handbook of Fire Protection Engineering. National Fire Protection Association, Bethesda, MD, 3rd edition, 2002

[12] Planck, M.; Ueber das Gesetz der Energieverteilung im Normalspectrum; Ann. Phys. IV (1901) 553-563

[13] Grosshandler, W. L.; RADCAL: A Narrow-Band Model for Radiation Calculations in a Combustion Environment. NIST TN 1402; April 1993